The International Journal of Advanced Manufacturing Technology (2022) 119:3013–3028
https://doi.org/10.1007/s00170-021-08587-x

ORIGINAL ARTICLE

Load capacity of single-lap adhesive joints made of 2024-T3 aluminium alloy sheets after shot peening

Władysław Zielecki[1] · Tomasz Trzepieciński[1] · Łukasz Bąk[2] · Ewelina Ozga[1]

Received: 29 August 2021 / Accepted: 15 December 2021 / Published online: 5 January 2022
© The Author(s) 2022

Abstract

The goal of the work reported was to determine the influence of selected shot peening parameters on the deflection of the Almen strip and the load capacity of single-lap adhesive joints made of 2-mm-thick aluminium alloy EN AW-2024-T3. Moreover, the research was aimed at checking the possibility of using the Almen strip deflection indicator to predict the load capacity of adhesive joints after shot peening. The analysis was carried out according to Hartley's PS/DS-P:Ha3 plan. The input factors were the shot peening parameters: treatment time t (60–180 s), ball diameter d_k (0.5–1.5 mm) and compressed air pressure p (0.3–0.5 MPa). It has been proved in this work that shot peening treatment of the outer surface of single-lap adhesive joints can be used to strengthen the joint. The maximum increase in the load capacity of the shot peened joints was 33.4%. It was observed that the load capacity of the joints decreases with an increase in the deflection of the Almen strip (in the assumed area of variability of technological parameters). Moreover, the results obtained indicate that the adoption of too intensive treatment, manifested in high values of deflection of the Almen strip, may weaken single-lap adhesive joints.

Keywords Almen strip · Adhesive joint · Aluminium alloy · Hartley's plan · Load capacity · Shot peening

1 Introduction

Single-lap adhesive joints offer many benefits, such as saving time, economising on costs, very high strength and good damping properties in comparison with other conventional joining processes [1, 2]. Ahmed and Tehami [3] and Gültekin et al. [4] showed that bond length, adhesive thickness, adherend thickness, curing conditions and joint end geometry are the factors that affect the strength of the adhesive joints. Surface treatment was the most important among these factors because it could influence the surface roughness and wettability of the adherend [5]. Moreover, the problem of fatigue in mechanical joining elements such as screws, fasteners and rivets, and their lower strength-to-weight ratios are successfully resolved by adhesive bonding technology [6, 7].

The shear stress distribution in the overlap zone in single-lap adhesive joints loaded in tension is not uniform. Maximum stresses are located at the ends of the adhesive layer. The changes in dimensions at the ends of the overlap (geometric notch) are one of the causes of uneven stress distribution. Another reason for this phenomenon is the differential straining of the adherends. The stresses are formed at the ends of the overlap owing to the differences in plastic properties of the adherend and adhesive [8–11]. The failure of the adhesive joint begins at the point where the stresses are the highest. Therefore, these stress peaks should be decreased in order to increase the strength of the joint [12].

One of the methods that allow the reduction in residual stresses in the edge zone of the overlap is the use of an adhesive with ductile behaviour and low modulus. Adhesives characterized by high flexibility and ductility are generally not strong. However, they deform plastically and provide a more uniform stress distribution than a rigid adhesive [12]. Another method is to apply an optimum adhesive layer. The peak values of the residual stresses increase with the decrease in adhesive thickness. One of the explanations for this phenomenon is that a thinner adhesive is more vulnerable to deformation than a thicker one [13]. The presence of the adhesive flash in the zone of stress concentration is

✉ Tomasz Trzepieciński
tomtrz@prz.edu.pl

[1] Department of Manufacturing and Production Engineering, Al. Powst, Rzeszow University of Technology, Warszawy 8, 35-959 Rzeszów, Poland

[2] Department of Materials Forming and Processing, Rzeszow University of Technology, Rzeszów, Poland

another factor reducing these stresses [14]. The positive effect of the adhesive flashes was observed, in particular in joints with small dimensions of the overlap [15].

The stresses in the near-edge zone can also be reduced by changing the geometry of the laps. These changes may include, for example, rounding adherend corners [16–18], tapering [16, 19, 20] and notching the adherends [21, 22]. Changing the adherends' geometry allows the peel stresses concentrated at the ends of the overlap to be reduced and, as a result, increases joint strength. However, these solutions are associated with an increase in the production costs of adhesive joints and may be troublesome in the case of processing thin sheets. A simple method that also allows stress peaks to be decreased and improves the strength of the adhesive joints is shot peening. Shot peening is one of the methods of dynamic burnishing. In this cold working process, the component surface is bombarded by small spherical particles which are propelled by a stream of compressed air [23–25]. The basic parameters influencing the efficiency of the shot peening process include: processing time, ball diameter, compressed air pressure, total number of balls in the working chamber and nozzle structure [26]. The intensity of the process can be determined by the value of the Almen strip deflection. Another method of controlling the process is assessing the degree of surface coverage with traces of the treatment [27].

As a result of shot peening, local plastic deformations are created and a compressive residual stresses field is formed in the near surface layers of the workpiece [24]. In addition, shot peening affects surface roughness and hardness. Therefore, it can be used to improve fatigue fracture resistance, hydrogen cracking fracture resistance and the life of stress corrosion [23, 27]. Moreover, as already mentioned, this treatment strengthens the adhesive joints. It introduces compressive residual stresses in the outer surface of the laps. These stresses deform and press the edge of the overlap against the bonded material. In the near-edge zone of the joint, a stress state is established in which the maximum principal normal stresses as well as the peel and tensile stresses are negative. Applying an external load to joints subjected to shot peening causes summation of the stresses caused by the external load and the stresses formed in the shot peening process. As a result, the principal normal stresses, tensile stresses and peel stresses decrease (Fig. 1) and the strength of the adhesive joints increases [26].

The positive effect of shot peening on the strength of adhesive joints has been proved in several studies [11, 28]. However, the effect of peening parameters on the adhesive joint strength is still controversial. Zielecki [26] investigated the effect of shot peening on the shear strength of S235JR steel adhesive joints made with Epidian 5 (CIECH Sarzyna S.A, Nowa Sarzyna, Poland) composition with PAC

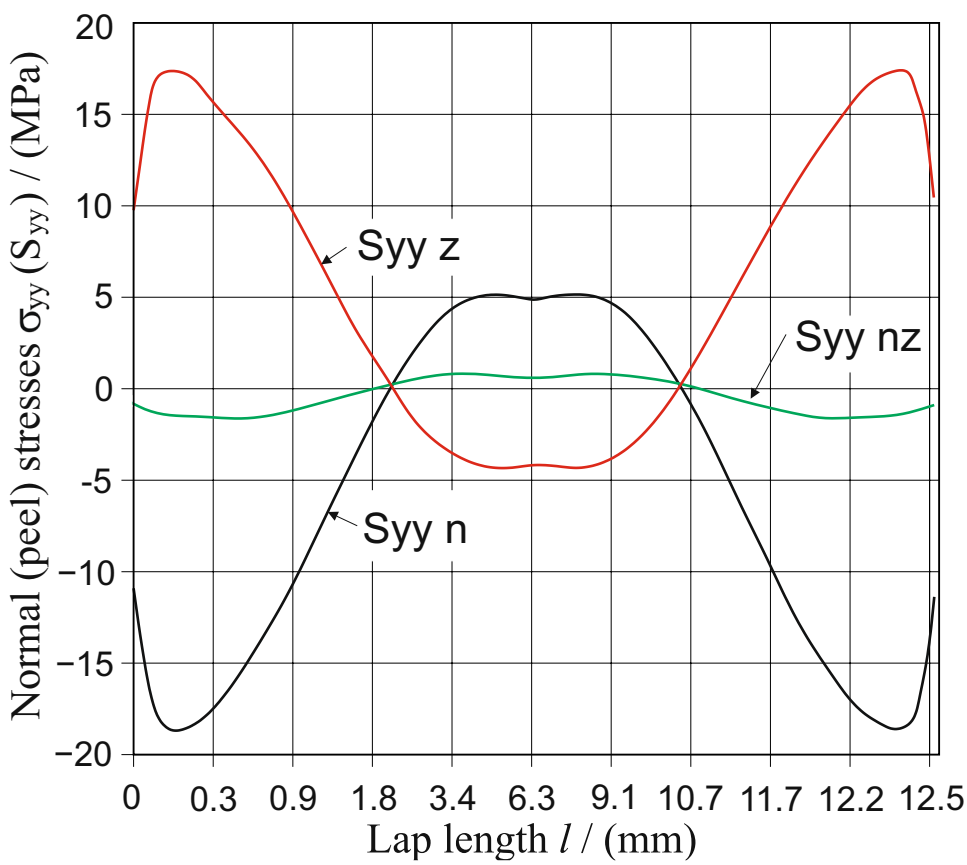

Fig. 1 Distribution of normal (peel) stresses σyy (Syy) in the middle layer of the adhesive joints: n—shot peened joints, z—joints loaded with external force $P = 2000$ N, nz—joints shot peened and loaded with external force $P = 2000$ [26]

hardener (flexible adhesive joint) and Epidian 5 composition with Z1 hardener (rigid adhesive joint). The treatment time was 60 s, the ball diameter was 2 mm, and the pressure was 0.35–0.55 MPa. For the samples with a flexible joint, a 17–27% increase in joint strength was observed. Moreover, it was found that the strength of the joints increases with increasing pressure. For the samples with a rigid joint, the strength of the joints increased by 93–112%.

According to the results presented by Korzyńska et al. [11], the shot peening treatment increases the strength of adhesive joints by 18–57%. The authors also showed that the strength of the joints is related to the state and magnitude of stresses in the samples treated with shot peening. The influence of shot peening on the strength of adhesive joints made of 2024 aluminium alloy was investigated in work [28]. The variable parameters in the treatment were: ball diameter (2–2.5 mm), pressure (0.2–0.3 MPa) and time (60–180 s). As a result of the shot peening, the load capacity of the test joints increased by 3.6–20.3%.

Shot peening can be used as one of the methods of increasing strength in adhesive joints. Moreover, this treatment has numerous advantages (low energy consumption, wide application, easy controllability, no waste in the form of shavings and dust). The impact of the shot peening process on the load capacity of adhesive joints is still little known. The analyses carried out so far are partial and mainly concern iron and titanium alloys. Therefore, it is reasonable to conduct further research in this direction, search for optimal parameters of shot peening and search for methods of evaluating the correctness of the process. Shot peening, along with other methods (alkaline degreasing, anodising, anodising combined with shot peening, laser treatment, sand blasting), is mainly used as the surface treatment method for preparing adherend surfaces for adhesive bonding. In this paper, the shot peening is used to increase the load capacity of adhesive joints by (i) creating compressive stresses in the outer layers of the single-lap adhesive joint and (ii) work hardening of the material. To the best of authors' current knowledge, similar studies, initiated by Zielecki [26] and investigated in later years [11, 28], are not reflected in the open literature.

The research presented in the article had two main goals. The first was to determine the influence of selected shot peening parameters on the deflection of the Almen strip and the load capacity of single-lap adhesive joints made of EN AW-2024-T3 aluminium alloy sheets. The second aim was to check whether it is possible to use the Almen strip deflection indicator to predict the load capacity of adhesive joints after shot peening. The tests were carried out according to three-leveled Hartley's polyselective quasi D (PS/DS-P: Ha3) plan, described in [29]. As part of the work, regression and correlation analysis was carried out on the relationship between the load capacity of adhesive joints and the process intensity.

2 Materials and methods

The single-lap adhesive joints were made of 2-mm-thick EN AW-2024-T3 aluminium alloy sheets. This alloy distinguishes itself through its high strength to weight ratio, good fatigue and high temperature resistance. However, it has low corrosion resistance and is non-weldable. The chemical composition is listed in Table 1.

The first step of the study was to prepare the surface for bonding. The adherend surface of the samples was subjected to abrasive blasting with 95A electrocorundate having a granularity of 0.27 mm. The abrasive blasting process parameters were: air pressure 0.7 MPa and time 30 s.

The average values of the roughness parameters of the surface prepared for gluing were Ra = 4.53 µm, Rz = 25.95 µm, Rq = 5.67 µm, Rku = 2.99, RSm = 0.141 mm. The surfaces were then degreased manually using acetone. Figure 2 shows a profilogram of the surface prepared for gluing.

The dimensions of the plates for making single-lap joints were 100 mm (length), 25 mm (width) and 2 mm (thickness). The length of the adhesive joint overlap was 12.5 mm. The joints were bonded with the use of EA3430 two-component epoxy adhesive (Loctite, Düsseldorf, Germany). It is a general-purpose adhesive suitable for poorly fitting and rough surfaces made from wood, metal, rigid plastics or ceramic. After applying a uniform layer of adhesive using an application comb for adhesives and joining the surfaces, the samples were placed in a mechanical device shown in Fig. 3a.

The mechanical device consisted of a set of levers at the end of which weights are mounted (Fig. 3b). This device allows one to glue six sets of specimens simultaneously. The samples were manually placed in the bearing insert (Fig. 3b). Then a manual lever was placed on the specimen

Table 1 Chemical composition of EN AW-2024-T3 aluminum alloy in wt.% [30]

Si	Fe	Cu	Mn	Mg	Cr	Ni	Zn	Ti	V	Others*	Al
max 0.50	max 0.50	3.8 - 4.9	0.30—0.90	1.2 - 1.8	max 0.10	-	max 0.25	max 0.15	-	max 0.05	remaining

*Others, total ≤ 0.15%

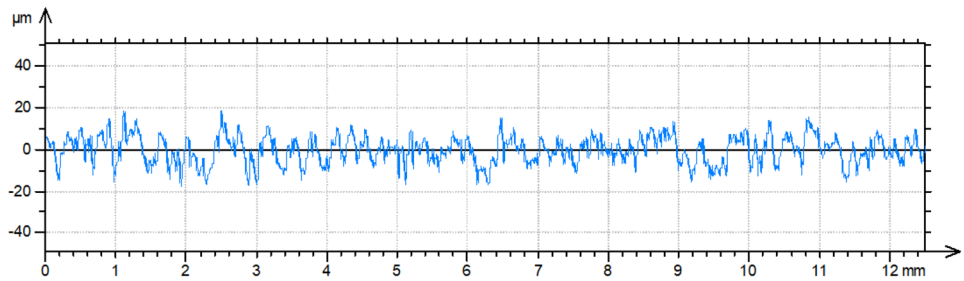

Fig. 2 Profilogram of the adherend's surface prepared for gluing

pack, at the end of which weights were placed manually. Thus, the jigging fixture allowed the samples to be laden with constant force using one-kilogram weights for each set of specimens. The samples were cross linked at 24 ˚C for 3 days. In this way, a reproducible thickness of the adhesive layer was ensured on all specimens. The thickness of adhesive determined as the average of 10 measurements was 0.09 mm (standard deviation 0.012 mm). An electronic slide caliper with an accuracy of 0.01 mm was used to measure the thickness of the adhesive layer on the basis of the difference in the thickness of the overlap joint and the thickness of the adherends.

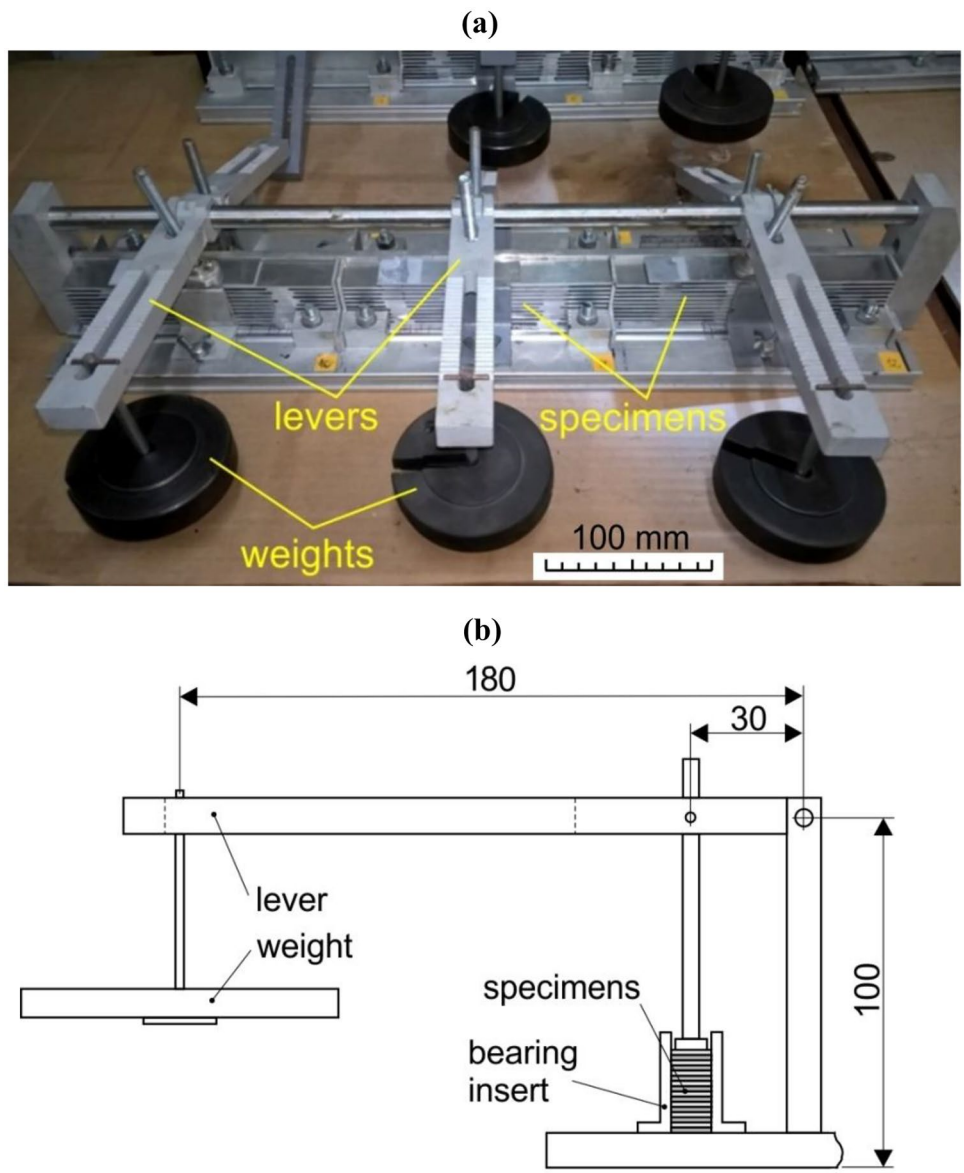

Fig. 3 (**a**) Samples placed in a mechanical device and (**b**) principle of operation (units in mm)

After cross-linking, the outer sides of the joints in the overlap zone (Fig. 4) were subjected to shot peening treatment. The rest of surfaces was protected during processing using covers (Fig. 5). The values of the shot peening parameters were based on the experience gained in previous studies and on the relevant literature [11, 28]. The distance between the nozzle and the specimen was 100 mm. The shot peening parameters for individual variants were selected according to the matrix of Hartley's PS/DS-P: Ha3 plan. The experiments were performed with three different values for the input factors: time t, ball diameter d_k and pressure of the compressed air p. The values of shot peening parameters for the individual variants are presented in Table 2, and the main values of the shot peening parameters (input factors), change intervals and coded values are presented in Table 3. Eight specimens were produced and tested for each variant.

The adhesive joints were subjected to a static tensile test on a Z030 (Zwick/Roell, Ulm, Germany) universal testing machine (Fig. 6). The samples were axially loaded at a speed of 5 mm/min until the joints were broken. The time between specimen shot peening and mechanical testing was 72 h. The force at break was taken as the load capacity of the joints P_t.

The tests also included an assessment of the shot peening intensity. The treatment intensity was determined using the value of the Almen strip deflection f_A. Type A2 control strips were used in the study. These plates are intended for medium process intensity, the thickness of the strips being 1.32 mm, hardness 44–50 HRC and flatness ± 0.038 mm. Only one side of the strips was shot peened. As a result of

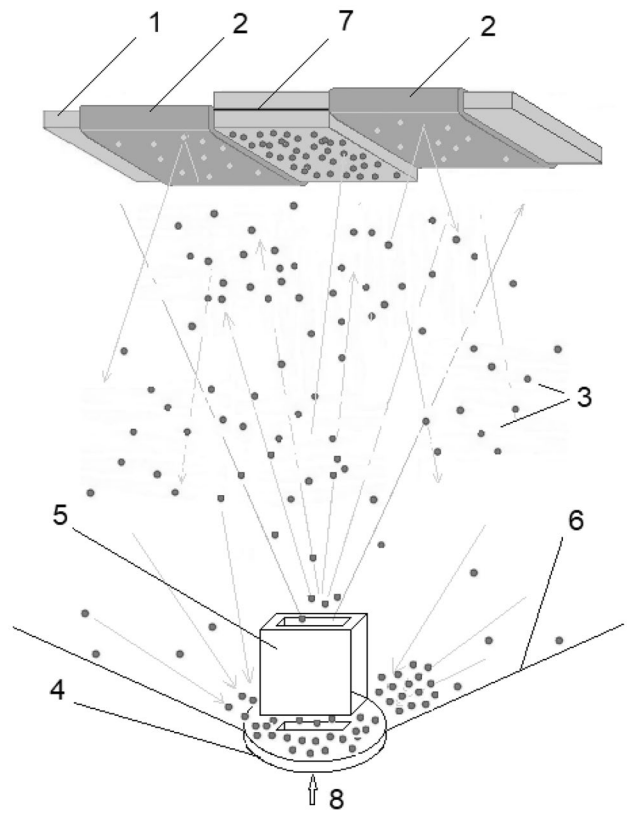

Fig. 5 Schematic illustration of the shot peening process: 1—specimen, 2—cover, 3—steel balls, 4—compressed air nozzle, 5—de Laval nozzle, 6—bottom of the working chamber, 7—adhesive, 8—compressed air supply

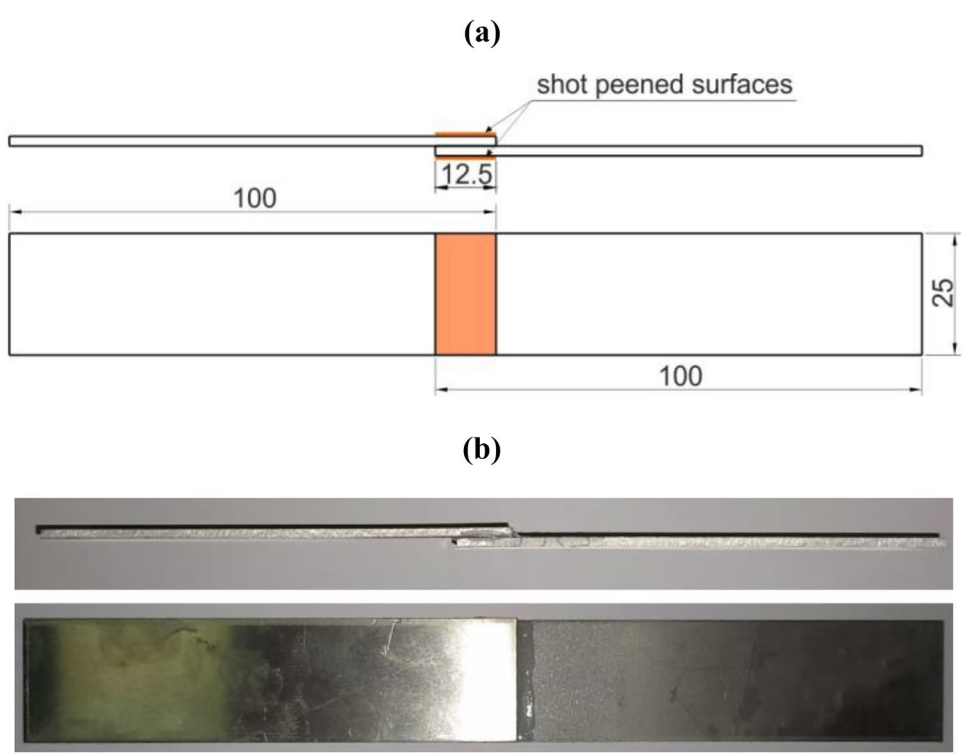

Fig. 4 (**a**) Drawing and (**b**) picture of specimen of an adhesive joint used in strength testing (units in mm)

Table 2 Values of shot peening parameters for individual variants

Variant	Shot peening parameters		
	Time t, s	Ball diameter d_k, mm	Pressure p, MPa
1	60	0.5	0.5
2	180	0.5	0.3
3	60	1.5	0.3
4	180	1.5	0.5
5	60	1.0	0.4
6	180	1.0	0.4
7	120	0.5	0.4
8	120	1.5	0.4
9	120	1.0	0.3
10	120	1.0	0.5
11	120	1.0	0.4

the shot peening process, compressive residual stresses were introduced to the surface layer of the strips. These stresses caused deflection of the strips. The amount of deflection was measured with a TSP-3B Almen Gage (Electronics Inc., Mishikawa, IN, USA) measuring device.

3 Results

3.1 Tensile test

Load–displacement curves for non-peened and peened specimen (variant 4) are shown in Fig. 7a, b respectively. The curves for variants 1–9 have a similar slope. At a displacement of 0.8 mm, the tensile force was equal to approximately 6000 N. In the case of variant 4, specimens no 4 and 7 showed significantly lower load capacity than the other specimens. This is a result of the dominant adhesive failure mechanism for these joints. The reasons for the occurrence of adhesive failure can be found in the incorrect preparation of the surfaces of the adhesively bonded elements. However, this also occurs in properly prepared joints, usually due to the high strength of the adhesive material in relation to the adhesive strength of the joint [31]. The slope of most of the curves for non-peened specimens (Fig. 7a) was smaller than in the case of variants 1–9. This means shot-peening increased the stiffness of the joints for these variants.

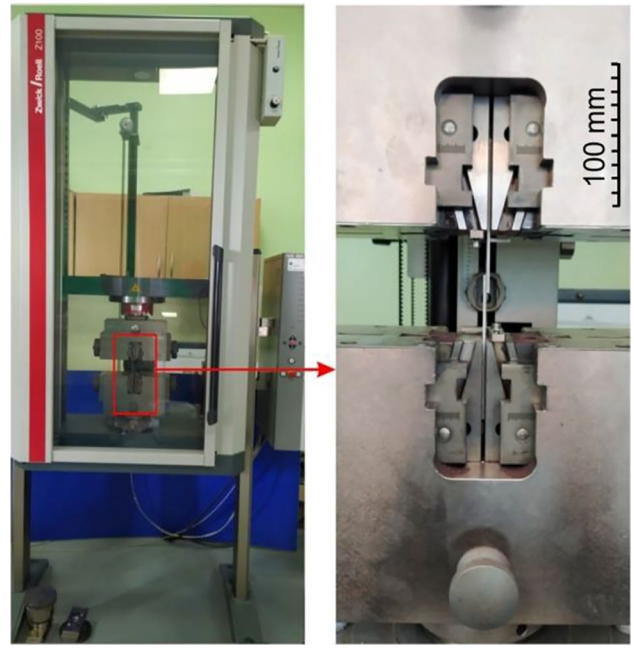

Fig. 6 Picture of the testing apparatus to estimate the joint load

A view of the fracture surfaces of the specimens after the tensile test is shown in Fig. 8. The failure mechanism was similar in different variants of the joints. We selected adhesive joints prepared according to variant 4 for presentation in order to show the difference of the failure mechanism for specimens showing $P_t = 883$ N and $P_t = 9707$ N.

In general, all the joints analysed showed a mixed adhesive-cohesive fracture mechanism. The samples made within the same variant were characterized by different proportions of adhesive and cohesive zones. Specimens with a greater share of adhesive failure zone showed reduced load capacity (Specimen 4 and 7 in Fig. 7b). The adhesive failure mechanism is the loss of adhesion

Table 3 Variability levels, main values, variability ranges and encoding methods of the factors for the model tests

Factor name	Value at the top and bottom level	Central values of input factors	Variation units	Method of encoding factor
Processing time t, s	+180 −60	$x_{10} = \frac{180+60}{2} = 120$	$\Delta_{x1} = \frac{180-60}{2} = 60$	$x_1 = \frac{t-60}{60}$
Ball diameter d_k, mm	+1.5 −0.5	$x_{10} = \frac{1.5+0.5}{2} = 1$	$\Delta_{x2} = \frac{1.5-0.5}{2} = 0.5$	$x_2 = \frac{d_k-1}{0.5}$
Pressure p, MPa	+0.5 −0.3	$x_{10} = \frac{0.5+0.3}{2} = 0.4$	$\Delta_{x3} = \frac{0.5-0.3}{2} = 0.1$	$x_3 = \frac{p-0.4}{0.1}$

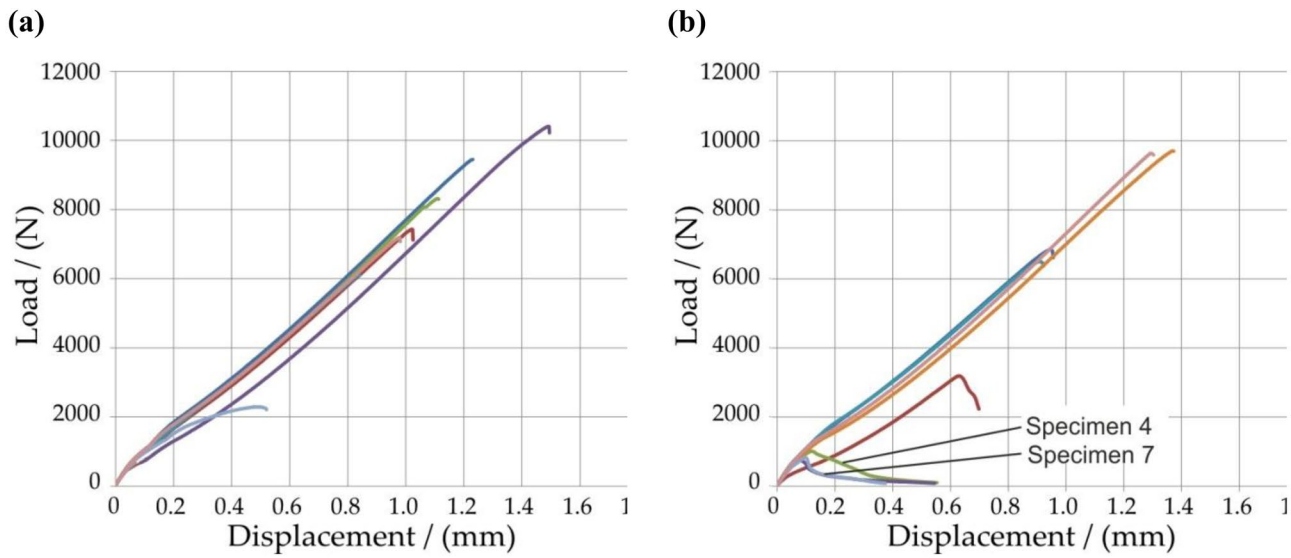

Fig. 7 Load–displacement curves for (**a**) non-peened specimen and (**b**) shot peened specimen (variant 7)

of the adhesive to the joined elements. A joint damaged as a result of the adhesive failure mechanism is characterized by complete detachment of the joined surfaces and a relatively low value of load capacity (Specimens 4 and 7 in Fig. 7b).

The specimens fractured due to the dominant share of the cohesive mechanism (for example Specimen 6 in Fig. 8) and showed a much higher load capacity. In general, the larger the cohesive failure area, the greater the joint strength. The cohesive failure mechanism results from the loss of load capacity of the adhesive material. It occurs when the stress state caused by an external load leads to the destruction of the adhesive layer. The cohesive failure mechanism is desirable in structural adhesive joints. A joint damaged in a cohesive manner is characterized by a delamination of the adhesive layer (Specimen 6 in Fig. 8). Most of the shot peened specimens with a wide range of process parameters have failed by a combined adhesive/cohesive failure mechanism. Thus, a clear relationship between the shot peening parameters and the failure mechanism cannot be established.

Conducting the experiment in accordance with the Hartley PS/DS-P:Ha3 plan allows us to determine a mathematical model of the object being tested. The model takes the form of a second-order polynomial (1):

$$y = b_0 + b_1x_1 + b_2x_2 + b_3x_3 + b_{11}x_1^2 + b_{22}x_2^2 + b_{33}x_3^2 + b_{12}x_1x_2 + b_{13}x_1x_3 + b_{23}x_2x_3 \quad (1)$$

where x_1 is the coded value for the treatment time t (s), x_2 the coded value for the ball diameter d_k (mm), x_3 the coded value for the pressure p (MPa) and $b_0, \ldots, b_{23}$—coefficients in the regression equation.

The critical value of the coefficients in the regression equation is used to determine the critical area. If the critical value is either greater than or equal to the calculated value, then the null hypothesis should be rejected and an alternative hypothesis adopted, according to which the tested coefficient has a statistically significant influence on the variable explained in the regression equation. Non-significance of specific coefficient justifies its removal from the regression equation. In the first step, the values of the coefficients in the regression equation were determined. Then, the coefficients were evaluated for significance. Calculations and significance assessment were performed in accordance with the methodology given in [29]. The results of the analyses are presented in Table 4.

Regression analysis allows to evaluate the amount of the error that estimates the explained variable (with the assumed probability) and allows to determine how much the linear regression model explains the observed variance of the dependent variable. Regression analysis aims to calculate such coefficients in the regression equation so that the model predicts well the value of the dependent variable and that the estimation error is as small as possible. If the coefficients in the regression model are statistically significant, the regression equation is useful to estimate the value of the dependent variable on the basis of the values of the explanatory variables (time t, ball diameter d_k and pressure p.

After the significance assessment of the regression equation coefficients and elimination of the non-significant coefficients, the following regression equation was obtained:

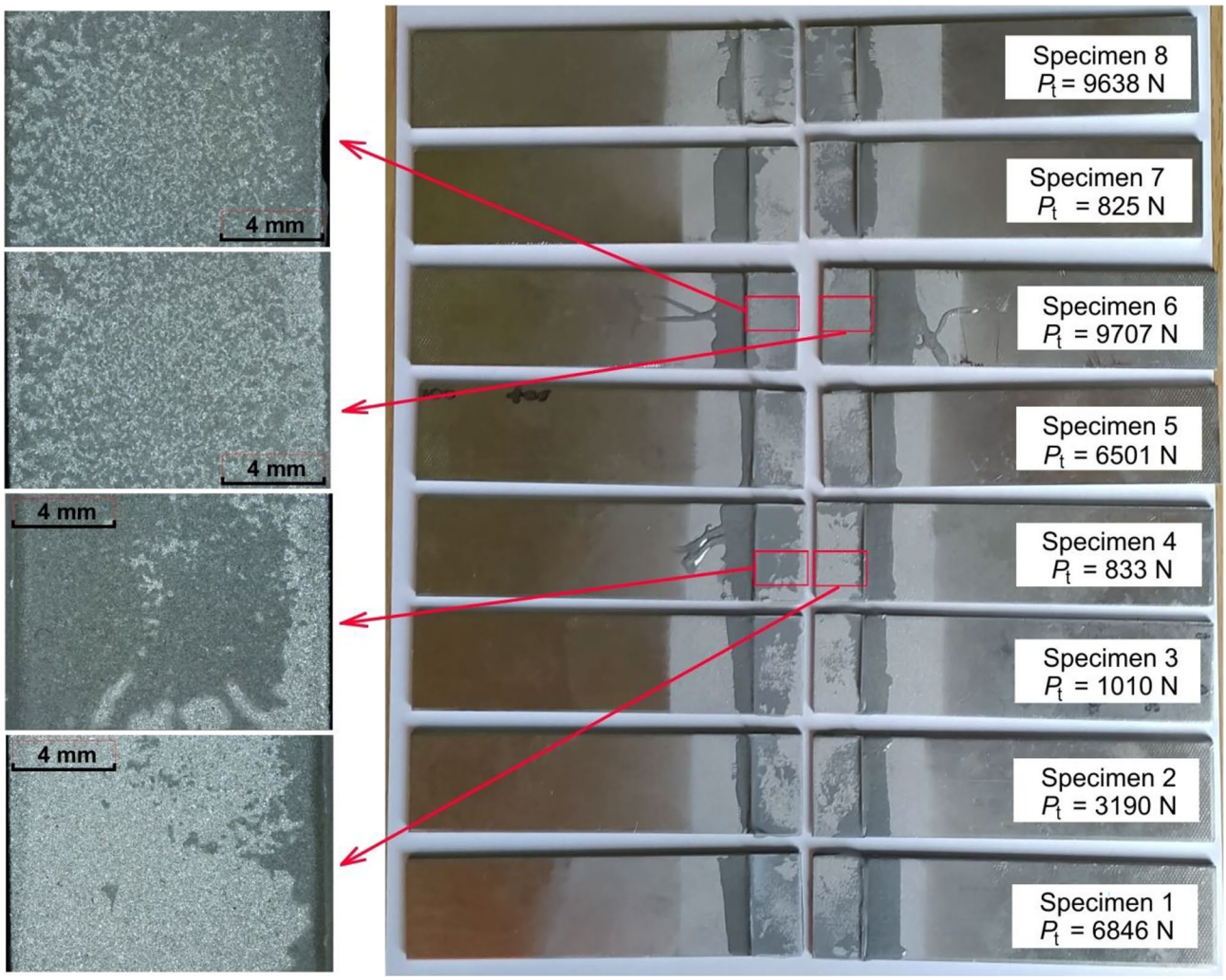

Fig. 8 View of the fracture surfaces of specimens (variant 4) after the tensile test

$$y = 8936 - 629.4x_1 - 1950.5x_2^2 - 1101.3x_2x_3 \quad (2)$$

Then, the regression equation was decoded. For this purpose, the coded values of the input factors have been replaced with the appropriate values from Table 3:

Table 4 Calculated values, critical values and significance of the regression coefficients in the regression equation describing the load capacity of joints

Coefficient	Critical value of the coefficient	Calculated value of the coefficient	Significance of coefficient	
b_0	701.2	8936.0	$\lvert b_0\rvert > b_{0kr}$	Significant
b_1	518.8	–629.4	$\lvert b_1\rvert > b_{kkr}$	Significant
b_2	518.8	–365.9	$\lvert b_2\rvert < b_{kkr}$	Non-significant
b_3	518.8	–275.7	$\lvert b_3\rvert < b_{kkr}$	Non-significant
b_{11}	816.8	94.1	$\lvert b_{11}\rvert < b_{kkkr}$	Non-significant
b_{22}	816.8	–1950.5	$\lvert b_{22}\rvert > b_{kkkr}$	Significant
b_{33}	816.8	63.9	$\lvert b_{33}\rvert < b_{kkr}$	Non-significant
b_{12}	635.5	–602.5	$\lvert b_{12}\rvert < b_{kkr}$	Non-significant
b_{13}	635.5	–572.1	$\lvert b_{13}\rvert < b_{kjkr}$	Non-significant
b_{23}	635.5	–1101.3	$\lvert b_{23}\rvert > b_{kjkr}$	Significant

$$y = 8936 - 629.4\left(\frac{t-120}{60}\right) - 1950.5\left(\frac{d_k-1}{0.5}\right) - 1101.3\left(\frac{d_k-1}{0.5}\right)\left(\frac{p-0.4}{0.1}\right) \quad (3)$$

After decoding and re-arranging, the regression equation takes a form:

$$y_{p_t} = -6417.6 - 10.49x_t + 24414.4x_{d_k} + 22026x_p - 7802x_{d_k}^2 - 22026x_{d_k}x_p \quad (4)$$

where y_{p_t} is the load capacity of the joint, x_t is the time variable, x_{d_k} is the ball diameter variable and x_p is the compressed air pressure variable. The regression equation thus obtained (4) is a mathematical model describing the effect of processing parameters on the load capacity of the single-lap adhesive joints made of EN AW-2024-T3 aluminium alloy sheets (for the variability of input parameters assumed in the research). This model is nonlinear.

Table 5 shows the values of the load capacity y_i of the adhesive joints determined in the static uniaxial tensile test. The static tensile tests wwere carried out for 12 variants (one variant for non-shot peened joint and 11 variants relating to shot peened joints). Strength tests were carried out for 8 adhesive joints from each variant.

The average value of the load capacity for specific variant was determined from the following formulae:

$$\bar{y}_i = \frac{\sum_{i=1}^{r} y_i}{r} \quad (5)$$

where y_i is the load capacity of the i-th joint in specific variant and r is the number of repetitions.

Variance of the measurement error can be determined on the basis of the following relationship:

$$S^2(y)_{(i)} = \frac{\sum_{i=1}^{r}\left(y_{ui} + \bar{y}_i\right)^2}{r-1} \quad (6)$$

where y_{ui} is the result of u-th repetition in i-th experiment.

The penultimate column in Table 5 lists the values of the load capacity of joints calculated from Eq. (4).

The results calculated from the equation agree with the experimental results; the Pearson's correlation coefficient is 0.85. A comparison of the load capacity of the joints determined experimentally and by Hartley's model is presented in Fig. 9.

The graphs shown in Fig. 10 present the influence of selected shot peening parameters on the load capacity of the adhesive joints. Based on the results in Fig. 10 and the results listed in Table 5, it can be concluded that the highest load capacity was achieved for variant 10 (the highest pressure, average time and average ball diameter) and for variant 6 (the longest time, average ball diameter

Table 5 Results of the static tensile test and mathematical modelling of the load capacity of single-lap adhesive joints *

Variant				Results of the load capacity measurements P_i, N								Results of the calculations			
No.	x_1	x_2	x_3	y_1	y_2	y_3	y_4	y_5	y_6	y_7	y_8	$\bar{y}_i$, N	$S^2(y)_i$ N^2	$\hat{y}_i$, N	$(\bar{y}_i - \hat{y}_i)^2$, N^2
NPV				8163	6164	6110	6535	7959	8396	7938	5372	7079	1343971		
1	-	-	+	5457	10109	10409	9065	7578	7570	7503	7635	8166	2624925	8716	303158
2	+	-	-	5487	10413	6597	6162	6163	5448	7007	10066	7168	3869761	5255	3659865
3	-	+	-	8658	8737	8807	9922	8589	6616	7011	7470	8226	1204818	8716	239997
4	+	+	+	6846	3190	1010	833	6501	9707	825	9638	4819	14721906	5255	190158
5	-	0	0	8387	7766	10018	8609	10008	8445	8340	8676	8781	652703	9565	615280
6	+	0	0	9154	10071	9080	8964	9967	9884	9195	8967	9410	226796	8307	1217506
7	0	-	0	6133	9332	5661	5774	5971	10722	6135	6310	7005	3660284	6985	369
8	0	+	0	9446	7428	8315	10404	6112	5599	2290	7186	7097	6338701	6985	12535
9	0	0	-	7976	7952	10808	8249	8966	8390	8513	8647	8688	847982	8936	61722
10	0	0	+	9553	7483	9273	9653	9237	10507	10815	9024	9443	1022434	8936	257127
11	0	0	0	8887	8863	6819	8624	8689	9132	9093	8957	8633	568118	8936	91787

* NPV – non-peened variant, $\bar{y}_i$ – average load capacity of the joint, $S^2(y)_i$ – variance of experimental results, $\hat{y}_i$ – load capacity of joint determined using regression equation (4), $(\bar{y}_i - \hat{y}_i)^2$ – variance determined using regression equation

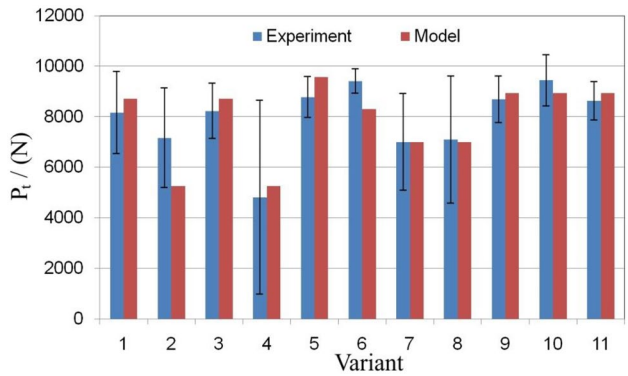

Fig. 9 Comparison of the load capacity of the joints determined experimentally and using regression equation (mathematical model)

and average pressure). The lowest value was achieved for variant 4, which has the highest values of the shot peening parameters. Low load capacity and the large dispersion of the test results for variant 4 may indicate that the processing parameters were too intensive. Too intense shot peening parameters could lead to damage to the adhesive or cohesive bonds and weaken the joint. Moreover, based on the graphs shown in Fig. 10 and the regression Eq. (4), it can be concluded that the influence of the ball diameter on the load capacity of the joints is nonlinear. The highest value of the load capacity (extreme) is observed for balls with a diameter of about 1 mm. In the case of peening time, a decrease in load capacity is observed with increasing time. The pressure is involved in two ways (it occurs independently and is related to the diameter of the balls). Nevertheless, it can be stated that an increase in pressure reduces the load capacity of the joints.

3.2 Almen strip deflection results

The treatment intensity was determined using the value of the Almen strip deflection f_A. Type A2 control strips were used in the study. A device called the Almen holder is used to fix the strip to the metal block with four bolts. Only one side of the strips was shot peened. Strips are mounted on their holders and subjected to the same peening conditions as the actual parts. The shots were fired to the surface of the specimens at an angle in order to avoid collision with the rebounding balls. As a result of the shot peening process, compressive residual stresses were introduced to the surface layer of the strips. These stresses caused deflection of the strips. The amount of deflection was measured with a TSP-3B Almen gage measuring device. Table 6 and Fig. 11 list the Almen strip deflection (f_A) measurement results and the results of mathematical model. In accordance with the Hartley's PS/DS-P:Ha3 plan methodology [29], the values of the coefficients of the regression equations were determined and their significance was

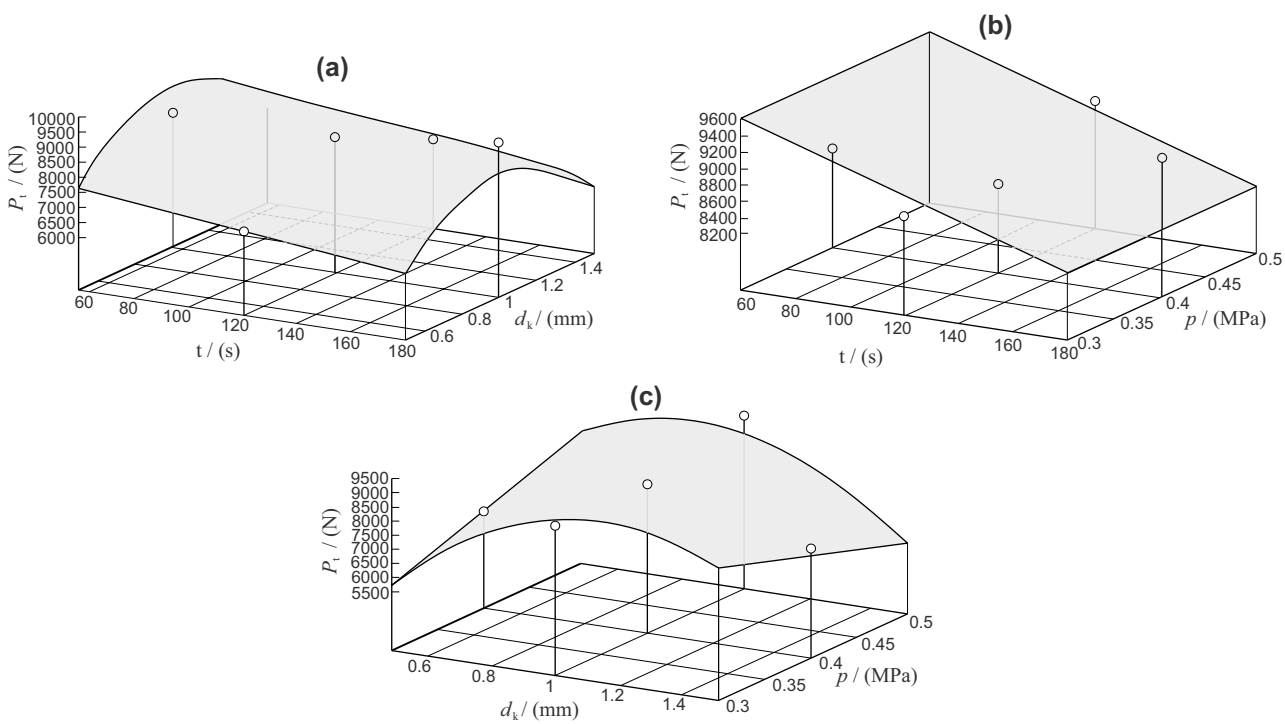

Fig. 10 Graphs showing: (**a**) the effect of time t and ball diameter d_k on load capacity P_t ($p = 0.4$ MPa), (**b**) the effect of time t and pressure p on load capacity P_t ($d_k = 1$ mm), (**c**) the effect of ball diameter d_k and pressure p on load capacity P_t (time t = 60 s)

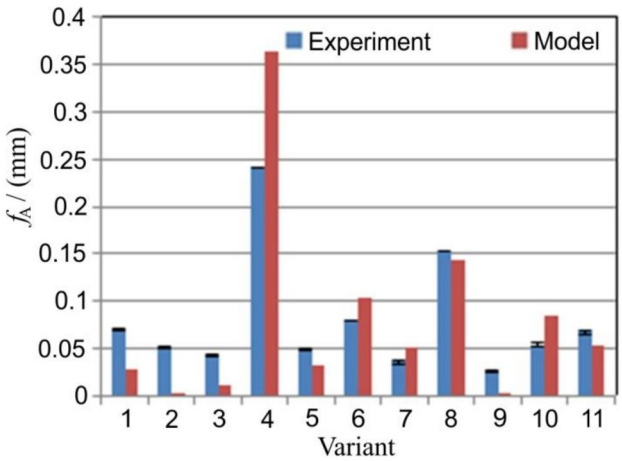

Fig. 11 Comparison of the Almen strip deflection f_A determined experimentally and predicted by Hartley's model

assessed. The results of the analyses are presented in Table 7. As mentioned in Sect. 3.1, if the critical value is either greater than or equal to the calculated value, then the null hypothesis should be rejected and an alternative hypothesis adopted, according to which the tested coefficient has a statistically significant influence on the variable explained in the regression equation. Non-significance of specific coefficient justifies its removal from the regression equation.

The average value of the Almen strip deflection for specific variant is determined from the following formulae:

$$\bar{y}_j = \frac{\sum_{j=1}^{r} y_j}{r} \tag{7}$$

where y_j is the Almen strip deflection of the j-th joint in specific variant and r is the number of repetitions.

Variance of the measurement error can be determined on the basis of the following relationship:

$$S^2(y)_{(j)} = \frac{\sum_{j=1}^{r} \left(y_{uj} + \bar{y}_j\right)^2}{r-1} \tag{8}$$

where y_{uj} is the result of u-th repetition in j-th experiment.

As a result of the significance assessment of the regression equation coefficients and the elimination of the non-significant coefficients, the following regression equation was obtained:

$$\begin{aligned} y = {} & 0.04194 + 0.035222x_1 + 0.046556x_2 + 0.041x_3 \\ & + 0.013535x_1^2 + 0.042871x_2^2 - 0.010467x_3^2 \\ & + 0.054667x_1x_2 + 0.040667x_1x_3 + 0.045x_2x_3 \end{aligned} \tag{9}$$

Then, the regression equation was decoded. For this purpose, the coded values of the input factors have been replaced with the appropriate values from Table 3:

$$\begin{aligned} y = {} & 0.054194 + 0.035222\left(\frac{t-120}{60}\right) + 0.046556\left(\frac{d_k-1}{0.5}\right) \\ & + 0.041\left(\frac{p-0.4}{0.1}\right) + 0.013535\left(\frac{t-120}{60}\right)^2 + 0.042871\left(\frac{d_k-1}{0.5}\right)^2 \\ & - 0.010467\left(\frac{p-0.4}{0.1}\right)^2 + 0.054667\left(\frac{t-120}{60}\right)\left(\frac{d_k-1}{0.5}\right) \\ & + 0.040667\left(\frac{t-120}{60}\right)\left(\frac{p-0.4}{0.1}\right) + 0.045\left(\frac{d_k-1}{0.5}\right)\left(\frac{p-0.4}{0.1}\right) \end{aligned} \tag{10}$$

After decoding and re-arranging, the following regression equation was obtained (11):

Table 6 Results of measurements of Almen strip deflection f_A*

Variant				Almen strip deflection fA, mm			Results of the calculations			
No	x_1	x_2	x_3	y_1	y_2	y_5	$\bar{y}_j$, mm	$S^2(y)_j$, mm^2	$\hat{y}_j$, mm	$(\bar{y}_j - \hat{y}_j)^2$, mm^2
1	-	-	+	0.070	0.070	0.072	0.071	0.000001	0.028	0.001790
2	+	-	-	0.050	0.052	0.052	0.051	0.000001	0.003	0.002902
3	-	+	-	0.042	0.042	0.044	0.043	0.000001	0.011	0.000973
4	+	+	+	0.242	0.242	0.242	0.242	0.000000	0.363	0.014700
5	-	0	0	0.048	0.050	0.048	0.049	0.000001	0.033	0.000261
6	+	0	0	0.080	0.080	0.080	0.080	0.000000	0.103	0.000527
7	0	-	0	0.034	0.036	0.036	0.035	0.000001	0.051	0.000230
8	0	+	0	0.152	0.152	0.152	0.152	0.000000	0.144	0.000070
9	0	0	-	0.028	0.026	0.026	0.027	0.000001	0.003	0.000573
10	0	0	+	0.052	0.054	0.056	0.054	0.000004	0.085	0.000944
11	0	0	0	0.070	0.066	0.066	0.067	0.000005	0.054	0.000173
Σ	-	-	-	-	-	-	0.87	0.000017	-	0.023144

* $\bar{y}_j$– Almen strip deflection f_A, $S^2(y)_j$– variance of experimental results, $\hat{y}_j$– Almen strip deflection f_A determined using regression Eq. (11), $(\bar{y}_j - \hat{y}_j)^2$—variance determined using regression Eq. (11)

Table 7 Calculated values, critical values and significance of the regression coefficients in the regression equation describing the Almen strip deflection

Coefficient	Critical value of the coefficient	Calculated value of the coefficient	Significance of coefficient	
b_0	0.000829	0.054194	$\lvert b_0 \rvert > b_{0kr}$	Significant
b_1	0.000614	0.035222	$\lvert b_1 \rvert > b_{kkr}$	Significant
b_2	0.000614	0.046556	$\lvert b_2 \rvert > b_{kkr}$	Significant
b_3	0.000614	0.041000	$\lvert b_3 \rvert > b_{kkr}$	Significant
b_{11}	0.000966	0.013535	$\lvert b_{11} \rvert > b_{kkkr}$	Significant
b_{22}	0.000966	0.042871	$\lvert b_{22} \rvert > b_{kkkr}$	Significant
b_{33}	0.000966	-0.010467	$\lvert b_{33} \rvert > b_{kkkr}$	Significant
b_{12}	0.000752	0.054667	$\lvert b_{12} \rvert > b_{kjkr}$	Significant
b_{13}	0.000752	0.040667	$\lvert b_{13} \rvert > b_{kjkr}$	Significant
b_{23}	0.000752	0.045000	$\lvert b_{23} \rvert > b_{kjkr}$	Significant

$$y_{f_A} = 0.688794 - 0.004848x_t - 0.828524x_{d_k} - 0.46598x_p + 0.000004x_t^2 + 0.171484x_{d_k}^2 - 1.0467x_p^2 + 0.001822x_{td_k} + 0.006778x_{tp} + 0.9x_{dk_p} \quad (11)$$

where y_{f_A} is the Almen strip deflection output variable, x_t is the time variable, x_{d_k} is the ball diameter variable and x_p is the compressed air pressure variable.

The regression equation thus obtained (Eq. (11)) represents the effect of processing time, ball diameter and compressed air pressure on deflection of the Almen strip (for the ranges of input parameters assumed in the research). The model is nonlinear. The penultimate column in Table 6 lists the values of deflection of the Almen strip calculated from the model (Eq. (11)). The results calculated from the equation agree with the experimental results. The Pearson's correlation coefficient is 0.95.

Figure 12 shows the influence of selected shot peening parameters on deflection of the Almen strip. It was observed that the highest values of deflection of the Almen strip were achieved for variant 4 which had the highest values of shot peening parameters and variant 8 which had the largest ball diameter, average time and pressure. The lowest value was observed for the lowest pressure, average time and ball diameter (variant 9). Moreover, on the basis of the graphs shown in Fig. 12 and the regression Eq. (11), it can be concluded

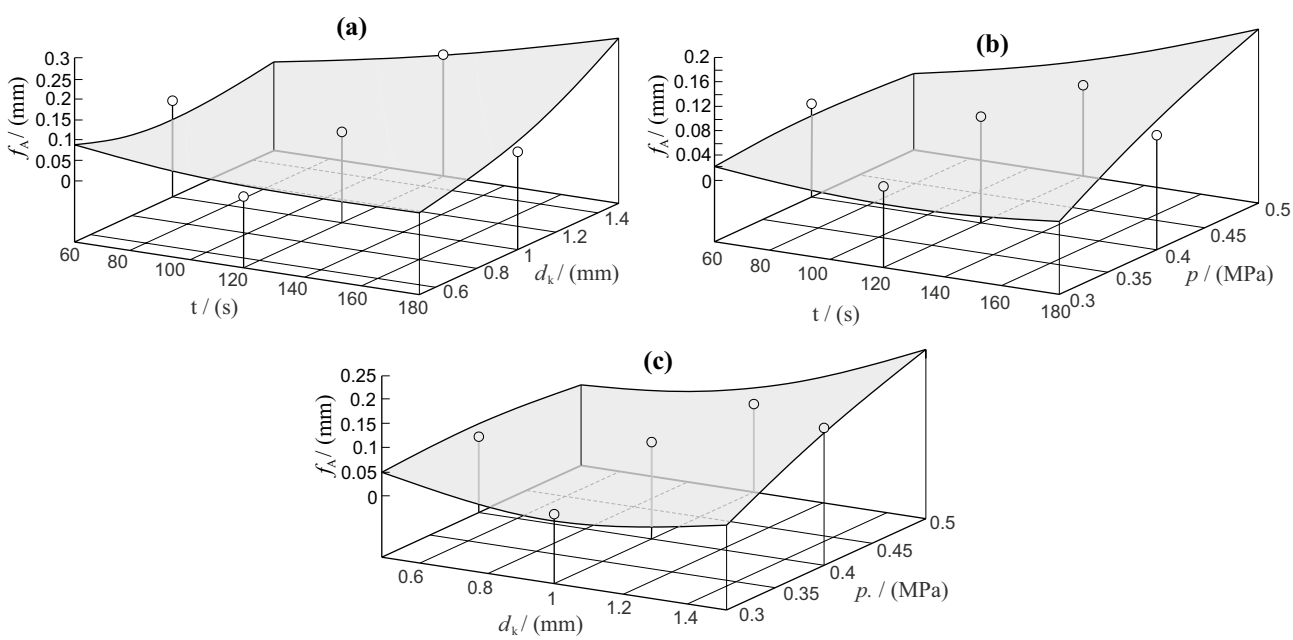

Fig. 12 Graphs showing: (**a**) the effect of the time t and ball diameter d_k on the deflection of the Almen strip f_A ($p = 0.4$ MPa), (**b**) the effect of time t and pressure p on deflection of the Almen strip f_A ($d_k = 1$ mm), (**c**) the effect of ball diameter d_k and pressure p on deflection of the Almen strip f_A ($t = 60$ s)

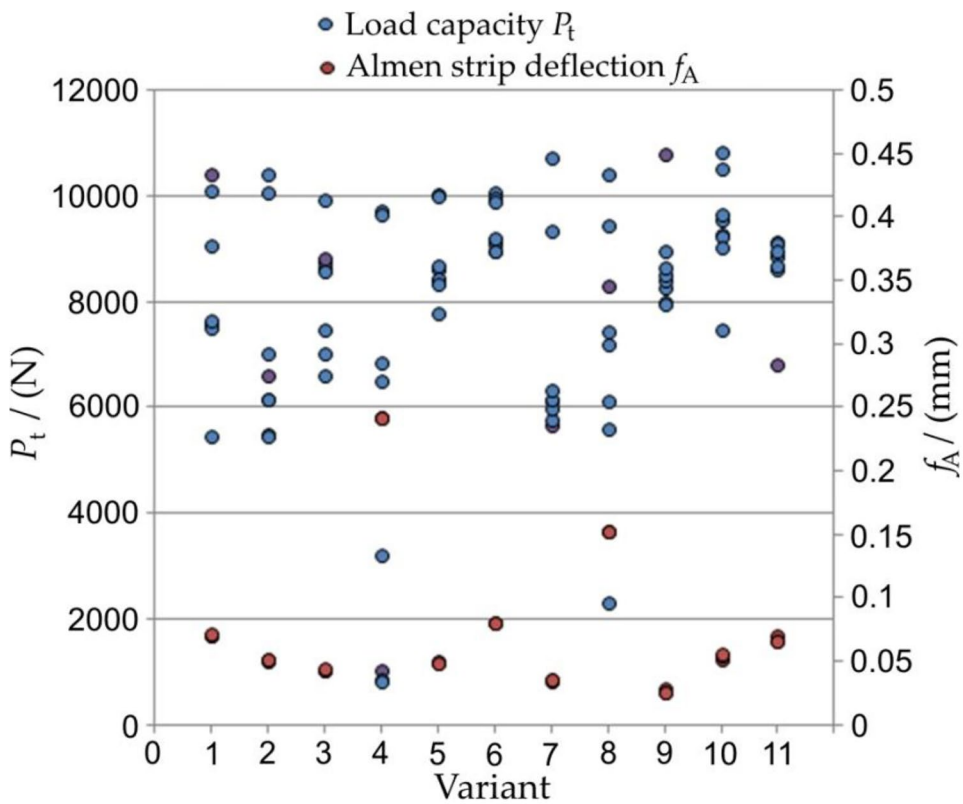

Fig. 13 Load capacity of joints versus deflection of the Almen strip

that the ball diameter and compressed air pressure greatly increase the value of the deflection of the Almen strip. Peening time had a smaller influence on the intensity of the process. Nevertheless, it can be concluded that increasing the shot peening time increases the deflection of the Almen strip.

4 Discussion

According to the analysis, it can be concluded that the shot peening treatment affects the load capacity of the adhesive joints and the deflection of the Almen strip. Figure 13 shows the values of the load capacity of the joint and the values of the deflection of the Almen strip obtained for individual processing variants, and Table 8 shows the highest and lowest load capacity of the joints after shot peening and the corresponding deflection values for the Almen strip.

Based on the diagram (Fig. 13) and Table 8, it can be concluded that high values of the technological parameters increase the intensity of processing and the degree of deflection of the Almen strip. However, high processing intensity does not translate into high joint strength.

Treatment variant number 4 had the greatest deflection of the Almen strip. Nevertheless, the load capacity of the joint for this variant is the lowest. It is 31.9% lower than the load capacity of the joints that were not subjected to shot peening. In this case, the shot peening treatment contributed to the weakening of the joints. The load capacity of the joints may have decreased rapidly as a result of too intensive treatment which damaged the cohesive or adhesive bonds. In the remaining shot peening variants of the treatment, an increase

Table 8 Comparison of load capacity in test and deflection of the Almen strip for shot peened and non-shot peened variants of the joints

Variant	Load capacity P_t, N	Almen strip deflection f_A, mm	Improved/decreased load capacity, %
Without shot peening treatment	7080	-	-
Shot peened—the best result (variant 10)	9443	0.054	33.4 (improved)
Shot peened—the worst result (variant 4)	4819	0.242	31.9 (decreased)

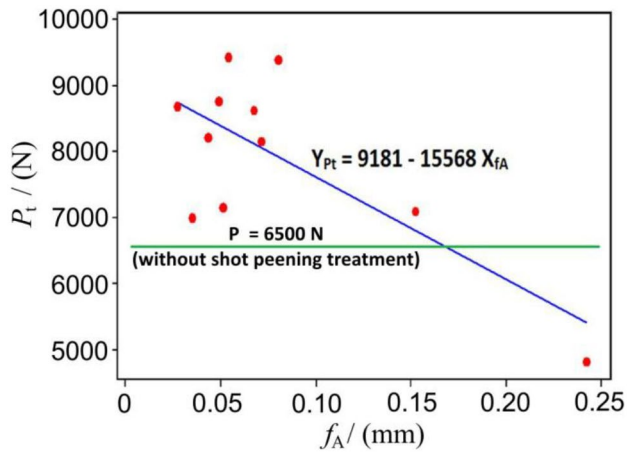

Fig. 14 Load capacity of joints P_t versus Almen strip deflection f_A

in the load capacity of the joints was observed. The greatest increase in load capacity was 33.4%.

The regression equation presented in the diagram (Fig. 14) describes the impact of the deflection of the Almen strip on the load capacity of the adhesive joints. Based on the assessment of the significance of the coefficients of the regression equation, it can be concluded that both coefficients are significant. The *p*-values in both cases are less than 0.05 and are as follows: for the constant term 0 and for the parameter $f_A = 0.01$. According to the regression equation, the load capacity of the joints decreases with Almen strip deflection (in the assumed area of variability of the input factors). This is confirmed by the value of the Pearson correlation coefficient, which is –0.733. The determination coefficient indicates that 54% of the load capacity results can be described by the regression equation presented in the diagram (Fig. 14). This means that the deflection of the Almen strip can be used to assess the load capacity of the adhesive joints after shot peening.

The results of the experimental tests presented in this paper may be supplemented by the results of previous studies of the authors [11, 26, 28, 32]. The plates treated using SP exhibited high compressive residual stresses in the outer zone. This results in a better stress distribution and tightening of the joint edge, thereby increasing the strength of the joint.

Shot peening was carried out exactly along the length of the overlap so that (i) the residual stresses had an effect on the entire adhesive joint and (ii) the maximum stresses occurred at the edge of the overlap [32]. Shot peening causes compressive residual stresses in the adhesive layer with the highest value at the edge of the overlap [32]. Shot peening on longer or shorter lengths than the overlap length would not provide the maximum edge stresses. SP at a greater length than the overlap length would also cause the plates to deform beyond the joint zone, which we wanted to avoid.

5 Conclusions

The results of the research show that the shot peening process can be successfully applied to strengthen adhesive joints. Moreover, the relationship was determined between the deflection arrow and the load capacity of the joints after shot peening. It has been proved that the shot peening treatment of the outer surface of joints in the overlap area can be used to strengthen adhesive joints. The maximum increase in the load capacity of the shot peened joints was 33.4%. The load capacity of the adhesive joints after shot peening can be predicted from the value of the deflection of the Almen strip. As far as varying the relevant input factors is concerned, the load capacity of the joints decreases with the increase in the deflection of the Almen strip. Therefore, aluminium alloys should be shot peened with lower values of the process parameters, which will result in lower values of Almen strip deflection and thus lower stresses.

Shot peening affects a small subsurface depth of the sheet metal. So, the greater the thickness of the sheet (with other SP parameters constant), the lower will be the effect of shot peening on the value of the load capacity compared to the non-peened adhesive joint. On the other hand, if the sheet thickness decreases, the beneficial effect of introducing compressive stresses in external layers of the joint will be visible up to a certain sheet thickness. Shot peening of a very thin sheet may cause its deformation.

Author contribution Władysław Zielecki involved in conceptualization; Łukasz Bąk and Ewelina Ozga took part in experiments; Władysław Zielecki, Tomasz Trzepieciński, Ewelina Ozga involved in data interpretation; Władysław Zielecki, Tomasz Trzepieciński, Ewelina Ozga took part in writing—original draft preparation; Władysław Zielecki and Tomasz Trzepiecinski involved in writing—review and editing. All authors read and approved the final manuscript.

Funding The authors declare that no funds, grants, or other support was received during the preparation of this manuscript.

Availability of data and material The raw/processed data required to reproduce these findings are not shared. The datasets generated during and/or analysed during the current study are available from the corresponding author on request.

Code availability Not applicable.

Declarations

Ethics approval The authors declare the compliance with the ethical standards.

Consent to participate Not applicable.

Consent for publication Not applicable.

Conflicts of interest The authors have no relevant financial or non-financial interests to disclose.

Open Access This article is licensed under a Creative Commons Attribution 4.0 International License, which permits use, sharing, adaptation, distribution and reproduction in any medium or format, as long as you give appropriate credit to the original author(s) and the source, provide a link to the Creative Commons licence, and indicate if changes were made. The images or other third party material in this article are included in the article's Creative Commons licence, unless indicated otherwise in a credit line to the material. If material is not included in the article's Creative Commons licence and your intended use is not permitted by statutory regulation or exceeds the permitted use, you will need to obtain permission directly from the copyright holder. To view a copy of this licence, visit http://creativecommons.org/licenses/by/4.0/.

References

1. Kushwah S, Nhatt M, Desai C, Parekh S, Joshi P (2021) A methodological study for the stress analysis to evaluate single lap adhesive joint. IOP Conf Series: Mater Sci Eng 1149:012012. https://doi.org/10.1088/1757-899X/1149/1/012012
2. Akhavan-Safar A, da Silva LFM, Ayatollahi MR (2017) An investigation on the strength of single lap adhesive joints with a wide range of materials and dimensions using a critical distance approach. Int J Adhes Adhes 78:248–255. https://doi.org/10.1016/j.ijadhadh.2017.08.009
3. Ahmed E, Tehami A (2018) Evaluation of Strength of Adhesively Bonded Metallic Single Lap Joint with Different End Geometries. SAE Technical Paper 2018:011238. https://doi.org/10.4271/2018-01-1238
4. Gültekin K, Akpinar S, Özel A (2014) The effect of the adherend width on the strength of adhesively bonded single-lap joint: Experimental and numerical analysis. Compos Part B: Eng 60:736–745. https://doi.org/10.1016/j.compositesb.2014.01.022
5. Feng Z, Zhao H, Tan C, Chen J, Wang Y, Chen B, Song X (2019) Modification of surface treatment on the strength of 30CrMnSiAsteel adhesively bonded joints. Mater Res Express 6:116521. https://doi.org/10.1088/2053-1591/ab4483
6. Raga DFO, de Sousa LMC, Infante V, da Silva LFM, Moreira PMGP (2016) Aluminium friction-stir weld-bonded joints. J Adhes 92(7–9):665–678. https://doi.org/10.1080/00218464.2015.1085860
7. Kadioglu F, Avil E, Ercan ME, Aydogan T (2018) Effects of different overlap lengths and composite adherend thicknesses on the performance of adhesively-bonded joints under tensile and bending loadings. IOP Conf Series: Mater Sci Eng 369:012034. https://doi.org/10.1088/1757-899X/369/1/012034
8. Aimmanee S, Preeda H (2017) Stress analysis of adhesive-bonded tubular-coupler joints with optimum variable-stiffness-composite adherend under torsion. Compos Struct 164:76–89. https://doi.org/10.1016/j.compstruct.2016.12.043
9. Ashcroft IA, Mubashar A (2018) Numerical approach: Finite element analysis, in: LFM. da Silva, A Öchsner (Eds.), Handbook of Adhesion Technology. Springer-Verlag, Berlin Heidelberg, 701–740. https://doi.org/10.1007/978-3-319-55411-2_25
10. Kavdir EÇ, Aydin MD (2020) The experimental and numerical study on the mechanical behaviors of adhesively bonded joints. Compos Part B 184:107725. https://doi.org/10.1016/j.compositesb.2019.107725
11. Korzynska K, Zielecki W, Korzynski M (2018) Relationship between residual stress and strength of single lap joints made of Ti6Al4V alloy, adhesively bonded and treated using pneumatic ball peening. J Adhes Sci Technol 32(17):1849–1860. https://doi.org/10.1080/01694243.2018.1450108
12. da Silva LFM, Marques EAS, Campilho RDSG (2018) Design rules and methods to improve joint strength. In Handbook of Adhesion Technology; da Silva, LFM, Öchsner A, Adams RD, Eds.; Springer-Verlag, Berlin Heidelberg, 773–810. https://doi.org/10.1007/978-3-319-55411-2_27
13. Her SC, Chan CF (2019) Interfacial stress analysis of adhesively bonded lap joint. Materials 12:2403. https://doi.org/10.3390/2Fma12152403
14. Kowalczyk A, Weisbrodt M, Schmidt B, Gziut K (2020) Influence of acrylic acid on kinetics of UV-Induced cotelomerization process and properties of obtained pressure-sensitive adhesives. Materials 13:5661. https://doi.org/10.3390/2Fma13245661
15. Petrie EM (2008) The fundamentals of adhesive joint design and construction: Function-specific construction is the key to proper adhesion and load-bearing capabilities. Metal Finish 106(11):55–57. https://doi.org/10.1016/S0026-0576(08)80314-5
16. Calik A (2016) Effect of adherend shape on stress concentration reduction of adhesively bonded single lap joint. Eng Rev 36:29–34. https://doi.org/10.1016/j.compositesb.2014.01.022
17. Zhao X, Adams RD, da Silva LFM (2011) Single lap joints with rounded adherend corners: Experimental results and strength prediction. J Adhes Sci Technol 25:837–856
18. Zhao Z, Adams RD, da Silva LFM (2011) Single lap joints with rounded adherend corners: Stress and strain analysis. J Adhes Sci Technol 25:819–836
19. Günther N, Griese M, Stammen E, Dilger K (2020) Loading capacity of adhesive joints regarding their manufacturing process. J Adv Join Proc 1:100020. https://doi.org/10.1016/j.jajp.2020.100020
20. Hart-Smith LJ (2018) Adhesively bonded joints in aircraft structures. In Handbook of Adhesion Technology, da Silva LFM, Öchsner A, Adms RD, Eds.; Springer-Verlag, Berlin Heidelberg, 1235–1284. https://doi.org/10.1007/978-3-642-01169-6_44
21. Bahrami B, Ayatollahi MR, Beigrezaee MJ, da Silva LFM (2019) Strength improvement in single lap adhesive joints by notching the adherends. Int J Adhes Adhes 95:102401. https://doi.org/10.1016/j.ijadhadh.2019.102401
22. Kanani AY, Hou X, Ye J (2020) The influence of notching and mixed-adhesives at the bonding area on the strength and stress distribution of dissimilar single-lap joints. Compos Struct 241:112136. https://doi.org/10.1016/j.compstruct.2020.112136
23. Lin Q, Liu H, Zhu C, Chen D, Zhou S (2020) Effects of different shot peening parameters on residual stress, surface roughness and cell size. Surf Coat Technol 398:126054. https://doi.org/10.1016/j.surfcoat.2020.126054
24. Sherafatnia K, Farrahi GH, Mahmoudi AH, Ghasemi A (2016) Experimental measurement and analytical determination of shot peening residual stresses considering friction and real unloading behavior. Mater Sci Eng A 657:309–321. https://doi.org/10.1016/j.msea.2016.01.070
25. Tan L, Yao C, Zhang D, Ren J, Shen X, Zhou Z (2020) Effects of different mechanical surface treatments on surface integrity of TC17 alloys. Surf Coat Technol 398:126073. https://doi.org/10.1016/j.surfcoat.2020.126073
26. Zielecki W (2008) Determinants determining the strength properties of adhesive joint. Habilitation Thesis, Technical University of Košice, Košice, 2008
27. Liu J, Yue Z, Geng X, Wen S, Yan W (2018) Long-life Design and Test Technology of Typical Aircraft Structures. National Defense Industry Press, Beijing, China
28. Zielecki W, Bąk Ł, Guźla E, Bucior M (2019) Statistic analysis of the influence shot peening parameters on the capacity of single lap adhesive joints from aluminium alloy 2024. Technol Automat Mont 1:30–34

29. Gupta AK, Kabe DG (2013) Design and Analysis of Experiments. World Scientific Publishing Company, Singapore
30. ASTM B209–96 (1996) Standard specification for aluminium and aluminium-alloy sheet and plate. ASTM International, West Conshohocken, PA, USA
31. Wojtczak E (2015) Strength analysis of single lap adhesive joint. Bachelor thesis. Gdansk University of Technology, Gdańsk, Poland
32. Zielecki W, Perłowski R, Trzepieciński T (2007) Analysis of the stress state in the weld of an overlap adhesive joint strengthened by the shot peening. Technol Automat Mont 1:31–33

Publisher's Note Springer Nature remains neutral with regard to jurisdictional claims in published maps and institutional affiliations.